A Brief Introduction to the Physical Basis for Electron Spin Resonance

In ESR measurements, the sample under study is exposed to a large slowly varying magnetic field and a microwave frequency magnetic field oriented perpendicularly to the applied field [1,2]. Usually the measurements are made at an *X* band: a microwave frequency $\nu \cong 9.5$ GHz.

An unpaired electron has two possible orientations in the large applied field and thus two possible orientation dependent energies. (From classical electricity and magnetism, the energy of a magnetic moment $\boldsymbol{\mu}$ in a magnetic field **H** is $-\boldsymbol{\mu} \bullet \mathbf{H}$.) Magnetic resonance occurs when the energy difference between the two electron orientations is equal to Planck's constant, *h*, times the microwave frequency. For the very simple case of an isolated electron, the resonance requirement may be expressed as

$$h\nu = g_0 \beta_e H \,, \qquad (1)$$

where $g_0 = 2.002319$ and β is the Bohr magneton, $eh/4\pi m_e$, where *e* is electronic charge and m_e is the electron mass. The Bohr magneton is 9.274015×10^{-28} J/G.

Expression (1) describes the resonance condition for an electron which does not otherwise interact with its surroundings. The structural information provided by ESR is due to deviations from this simple expression. For relatively simple trapping centers, including all which have been studied in MOS systems, these deviations are due to spin-orbit coupling and electron–nuclear hyperfine interactions.

A. Spin-orbit coupling

The deviations from expression (1) due to spin orbit coupling come about because a charged particle, the electron, is traveling in an electric field due to the nuclear charge. It therefore experiences a magnetic field $\mathbf{B}=\mathbf{E}\times\mathbf{v}/c^2$, where **E** is the electric field, **v** is the velocity, and *c* is the speed of light. The spin-orbit interaction may be understood *qualitatively (*and *only* qualitatively) in terms of the Bohr picture: an electron moves about the nucleus in a circular orbit. It would appear to an observer on the electron that the positively charged nucleus is in a circular orbit about the electron. (It appears to an unsophisticated observer on earth that the sun is in a circular orbit about the earth.) The nucleus thus generates a local magnetic field which would scale with the

electron's orbital angular momentum, **r**x**p**, and with the nuclear charge. One would thus correctly surmise that spin-orbit coupling interactions increase with increasing atomic number and orbital angular momentum quantum number. This spin-orbit interaction is schematically illustrated in figure 2. (Note: Figure 2 is intended to provide only a qualitative approximation of reality.)

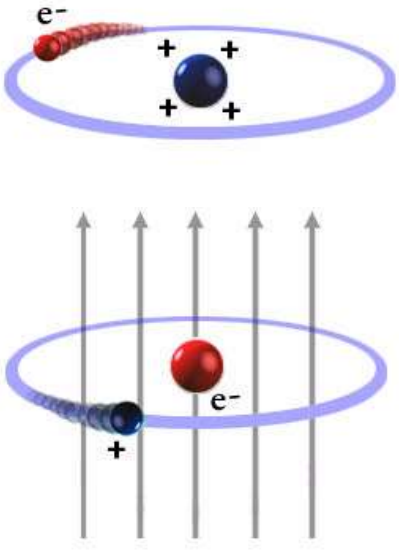

Figure 2. (a) An electron orbiting a nucleus in the (not quite right but illustrative) Bohr picture (b) An observer on the electron observes the motion of the nucleus around the electron. This results in a current around the electron and a local magnetic field. The local field increases with nuclear charge and increasing electron orbital angular momentum. Therefore, this contribution to the local field reflects the chemical nature of the site.

In solids, the spin-orbit interaction is ''quenched'' but a second order effect appears from excited states. This effect scales with the applied magnetic field and depends on the orientation of the paramagnetic defect in the applied magnetic field. The spin-orbit coupling may thus be included in the ESR resonance condition by replacing the constant g_0 of expression (1) with a second rank tensor g_{ij} . The symmetry of this tensor reflects the symmetry of the paramagnetic center. Under some circumstances, the symmetry of the tensor may permit identification of the defect under study.

Perturbation theory allows calculation (with modest accuracy) of the *g* tensor for the simple defects. The components of the *g* tensor are given by

$$g_{ij} = g_0\delta_{ij} - 2\lambda\sum_k \frac{<\alpha \mid L_i \mid k><k \mid L_j \mid \alpha>}{(E_k - E_\alpha)}. \qquad (2)$$

Here g_0 is the free electron value, λ the atomic spin-orbit coupling constant, L_i and L_j are angular momentum operators appropriate for the *x*, *y*, or *z* directions, and the summation is over all excited states *k*. State $|\alpha>$ and energy E_α correspond to the paramagnetic ground state of the system. The *g* tensor can often, by itself, provide structural information if the system under study contains nuclei of significantly different charge. The atomic spin orbit coupling constant, as figure 2 suggests, is a very strong function of nuclear charge. Thus a germanium dangling bond spectrum likely yields a much larger range of *g* tensor components than a silicon dangling bond.

B. Electron-nuclear hyperfine interactions

The other important source of deviation from expression (1) is the hyperfine interaction of the unpaired electron with nearby nuclei. Certain nuclei have magnetic moments; some important examples in semiconductor device materials are 7.8% of germanium nuclei, ^{73}Ge (spin 9/2), 4.7% of silicon nuclei, ^{29}Si (spin ½), almost 100% of hydrogen nuclei, ^{1}H (spin ½), as well as essentially 100% of phosphorous nuclei, ^{31}P (spin ½). The near 100% abundant ^{14}N nucleus has a spin of 1. A spin 1/2 nucleus has two possible orientations in the large applied field; a spin 1 nucleus three possible orientations. Each nuclear moment orientation corresponds to one local nuclear moment field distribution.

We envision the nuclear moment interacting with an unpaired electron residing in a wave function which is a linear combination of atomic orbitals (LCAOs). For intrinsic defects in SiGe and related systems, the most important cases almost certainly involve *s*- and *p*-type wave functions. (For defects involving transition metal impurities, analysis will be somewhat more complicated but the basic principles are the same.) The LCAO for an unpaired electron can be written as

$$|\alpha\rangle = \sum_n a_n \{c_s|s\rangle + c_p|p\rangle\}, \qquad (3)$$

where $|s\rangle$ and $|p\rangle$ represent the appropriate atomic orbitals corresponding to the *n*th site, a_n^2 represents the localization on the *n*th site, and c_s^2 and c_p^2 represent, respectively, the amount of *s* and *p* character of the wave function on the *n*th atomic site.

For a site in which the unpaired electron is reasonably well localized at a single atom, the analysis is particularly simple. To first order we can interpret ESR spectra from such a site in terms of *s*/*p* hybridized atomic orbitals localized at that central atom. (The generalization to a defect wave function involving significant sharing by several atoms is very straightforward.[1])

The electron nuclear hyperfine interaction of an electron in a *p* orbital is anisotropic: it corresponds to a classical magnetic dipole interaction as schematically illustrated in Fig. 3. The interaction is strongest when the field is parallel to the symmetry axis. The sign of the interaction changes and the magnitude is decreased by one half when the field is perpendicular to the symmetry axis. When the electron and nuclear moments are aligned by a strong magnetic field in the *z* direction, a reasonable assumption for work discussed in this appendix, only the *z* component of the dipolar field is important, because the interaction energy involves a dot product. $-\mu \bullet \mathbf{H}$. This *z* component, $g_n\beta_n(1\text{-}3\cos^2\theta)r^{-3}$, is averaged over the electronic wave function to produce the dipolar contribution,

$$\text{Dipolar contribution} = -g_n\beta_n\left\langle\frac{1-3\cos^2\theta}{r^3}\right\rangle. \qquad (4)$$

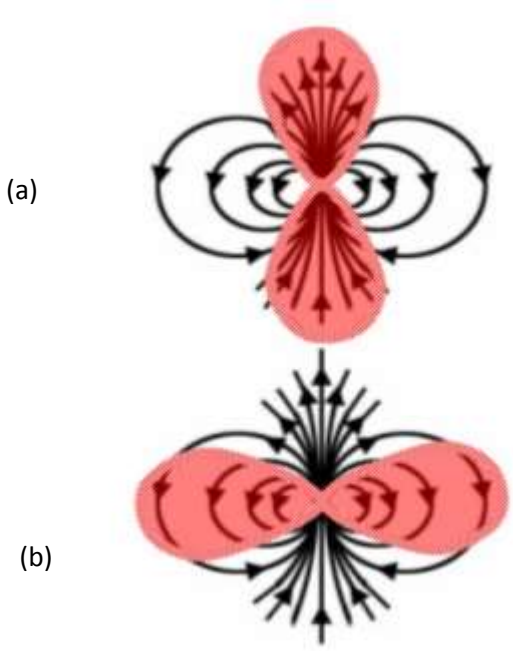

Figure 3. Interaction of the nuclear moments dipole field (lines) with the p orbital electron (shaded areas). In (a) the applied field, and thus the nuclear moment, is aligned parallel to the orbital symmetry axis. In (b) the applied field, and thus the nuclear moment, is aligned perpendicular to the orbital symmetry axis.

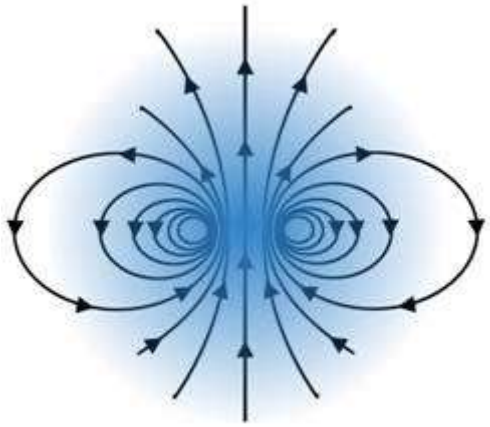

Figure 4. Interaction of the nuclear moments dipole field (lines) with the p orbital electron (shaded areas). The interaction of the electron and the applied magnetic field is axially independent because of the spherical symmetry of the s orbital.

The electron–nuclear hyperfine interaction of an electron in an *s* orbital is isotropic. This interaction is illustrated in Fig. 4. The figure shows why the interaction is isotropic. The spherical symmetry of the orbital results in zero interaction with this field except for a spherical region about the nucleus with a radius of an imaginary current loop generating the nuclear moment's field. Since the *s* orbital has a nonzero probability density at the nucleus, a large isotropic interaction results. The *s* orbital hyperfine interaction can also be computed from an elementary electricity and magnetism calculation: the magnetic field at the center of a current loop of radius *a* is given by $2\mu/a^3$, where m is the magnetic moment of the current loop. The probability density of the electron varies little over the volume of the nucleus; take it to be constant, $|\alpha(0)|^2$. Considering then only the fraction of the electron wave function at the nucleus, to be $\frac{4}{3}\pi a^3|\alpha(0)|^2$, the interaction would be

$$A \text{ (isotropic)} = \left(\frac{4}{3}\pi a^3|\alpha(0)|^2\right)\left(\frac{2\mu}{a^3}\right). \qquad (5)$$

The magnetic moment of the nucleus is the nuclear g factor, g_n, times the nuclear Bohr magneton, β_n. Thus, the isotropic or Fermi contact interaction is given by

$$A_{\text{iso}} = \frac{8\pi}{3} g_n \beta_n \left|\alpha(0)\right|^2, \qquad (6)$$

where $\left|\alpha(0)\right|^2$ represents the unpaired electron probability density at the nucleus.

Both isotropic and anisotropic hyperfine interactions are likely present for quite a few of the defects to be observed in SiGe systems. This is so because the unpaired electron wave functions generally involve both *p*-orbital and *s*-orbital character, and in some cases d-orbital character as well. The hyperfine interactions, like the spin-orbit interactions, are expressed in terms of a second rank tensor. In many cases, to a pretty good approximation, the centers have axially symmetric wave functions and thus an axially symmetric tensor is appropriate.

With the magnetic field parallel to the *p* orbital symmetry axis, the anisotropic coupling of Eq. (4) yields $(4/5)\, g_n \beta_n \left\langle r^{-3} \right\rangle$; the field perpendicular to the symmetry axis results in an interaction of half the magnitude and opposite sign -(2/5) $g_n \beta_n \left\langle r^{-3} \right\rangle$. This result is intuitively satisfying and consistent with the sketches of Fig. 3.

The components of the hyperfine tensor correspond to sums of the isotropic and anisotropic interactions for the applied field parallel and perpendicular to the unpaired electron's orbital symmetry axis:

$$A_{\parallel} = A_{\text{iso}} + 2A_{\text{aniso}}; \qquad (7)$$

$$A_{\perp} = A_{\text{iso}} - A_{\text{aniso}}, \qquad (8)$$

where

$$A_{\text{aniso}} = \frac{2}{5} g_N \beta_N \left\langle r^{-3} \right\rangle. \qquad (9)$$

For a paramagnetic center with a specific orientation (designated by the angle θ between the symmetry axis and the applied field vector) the resonance condition is

$$H = H_0 + M_1 A, \tag{10}$$

where $H_0 = h\nu / g\beta_e$, and M_1 is the nuclear spin quantum number,

$$g = (g_{\parallel}^2 \cos^2\theta + g_{\perp}^2 \sin^2\theta)^{\frac{1}{2}} \tag{11}$$

and

$$A = (A_{\parallel}^2 \cos^2\theta + A_{\perp}^2 \sin^2\theta)^{\frac{1}{2}} \tag{12}$$

Equations (10)–(12) and only moderately more complex general case expressions provide a very straightforward basis for analyzing ESR results for defects with a specific orientation with respect to the applied magnetic field.

The description of ESR spectra of defects within a poly-crystalline or amorphous film, such as an SiO_2 passivating layer, is more complex but still comprehensible. All defect orientations are equally likely and, due to the lack of long range order, slight differences in local defect geometry may be anticipated. The presence of defects at all orientations leads to the continuous distribution of both g and A values from $g_{\parallel}$ and $A_{\parallel}$ to $g_{\perp}$ and $A_{\perp}$. Differences in local geometry may also lead to slight defect-to-defect variations in $g_{\parallel}$, $g_{\perp}$, $A_{\parallel}$, and $A_{\perp}$.

(a) (b)

Figure 5. (a) Randomly oriented "dangling bond defects" lead to a relationship with any particular direction which is (b) not random at all. Many more dangling bonds point in a direction perpendicular to an axis than parallel to it. Thus, the ESR pattern of a random array of defects will yield a weak signal corresponding to the ESR parameters for the field parallel case and a strong signal for the field perpendicular case.

Both of these complications are relatively easy to deal with. The random distribution of defect orientation can be dealt with easily in terms of analytical expressions found in most ESR textbooks. Again, let's think about the somewhat simplified case of an axially symmetric defect wave function. (The most general lowest possible symmetry case is a logical extension of the higher symmetry case and is well understood.) For axially symmetric centers, far fewer centers will have the symmetry axis parallel to the applied field than perpendicular to it; thus the ESR spectrum intensity will be far stronger at the $A_{\perp}$ and $g_{\perp}$ values than at $A_{\parallel}$ and $g_{\parallel}$.) The slight defect-to-defect variations in *g* and *A* values lead to broadening of the line shapes anticipated for unbroadened tensor components. (The process is illustrated in Fig. 6.)

The evaluation of ESR hyperfine tensor components allows for a reliable and moderately precise identification of the unpaired electron's wave function.

A little common sense usually allows one to identify the magnetic nuclei involved in observed hyperfine interactions. (Common sense involves inspection of the fraction of the spectrum is split by the hyperfine lines, counting the number of hyperfine lines, if possible evaluating the symmetry of the defect spectrum…) Having identified the nuclear species involved, a first order analysis of the unpaired electron wave function is extremely straightforward in terms of the LCAO picture. For defects in a crystalline environment, Eq. (12) can be fit to the ESR spectrum for multiple orientations. (For more complex defects, the extension of Eq. (12) to the most general case is reasonably straightforward.[1]) For simple defects in a polycrystalline environment one may fit the appropriately broadened analytical expressions to the ESR spectra to yield $A_{\perp}$ and $A_{\parallel}$. (This process is illustrated in Fig. A5.) By applying Eqs. (7) and (8) to this result, one may then obtains the isotropic and anisotropic coupling constants A_{iso} and A_{aniso} .

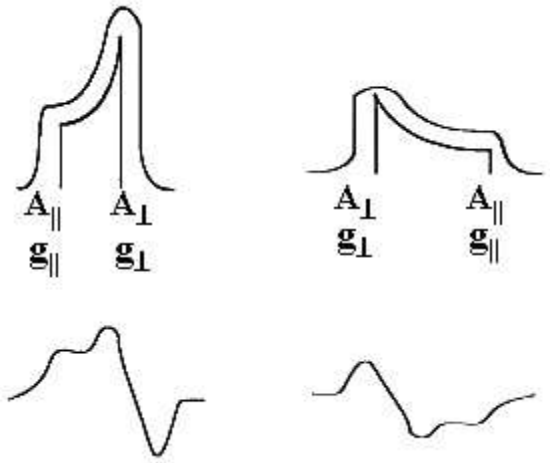

Figure 6. A schematic plot of ESR amplitude versus magnetic field corresponding to a site with axially symmetric g and hyperfine tensors and a spin-1/2 nucleus in a polycrystalline material, such as a polycrystalline thin film of SiGe. Note that the breadth of the lines depends on the range of variation in the g and hyperfine tensors.

Tabulated values of A_{iso} and A_{aniso} calculated for 100% occupation probability can then be utilized to determine the hybridization and localization of the electronic wave functions. For example, the isotropic and anisotropic coupling constants for an electron 100% localized in a silicon *s* and *p* orbital are, respectively, a_o=1639.3 G and b_o=40.75 G. In Fig. 7, we illustrate an ESR trace of the *E*' center, the dominating deep hole trap in high quality thermally grown oxides on silicon.

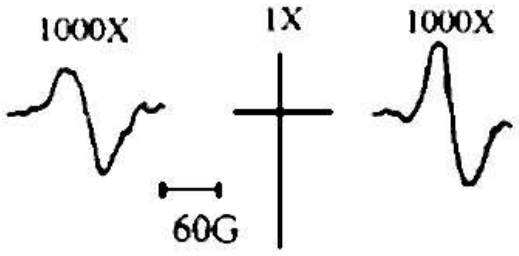

Figure 7. The ESR pattern of E' centers from SiO_2. The strong central peak (with about 95% of the total integrated intensity) corresponds to the 95% abundant ^{28}Si non-magnetic nuclear sites. The two weaker side peaks (with a combined intensity of about5%) are due to the ^{29}Si magnetic nuclei sites which are about 5% abundant.

An application of the analysis schematically indicated in Fig. 6 indicates that A_{iso}=439 G and $A_{aniso=}$22 G. If the electron were 100% localized in a silicon *s* orbital, we would expect an isotropic coupling constant of a_o =1639.3 G. We measured 439 G; thus the orbital has 439/1639 $\cong$ 27%*s*. If the electron were 100% localized in a silicon *p* orbital we would expect $A_{aniso}=b_o$=40.75 G. We measured $\cong$ 22 G; thus, the orbital has 22/40.75 $\cong$ 54%*p*. The analysis indicates a localization on the center silicon of about (54+27)=81%. Although the crude analysis just discussed is not extremely precise it is, to first order, *quite* reliable. One should realize that the isolated atomic values obtained for a_o and b_o are themselves only moderately accurate and that placing an isolated atom in a matrix of other atoms will inevitably alter the constants somewhat. Nevertheless, a straightforward analysis of hyperfine parameters provides moderately accurate measurement of hybridization and localization.

*References in text can be found on page labeled "*References*" on website*